

2022

# Parietal cell distribution informs gastric bypass procedure

---

<https://hdl.handle.net/2144/45650>

*"Downloaded from OpenBU. Boston University's institutional repository."*

BOSTON UNIVERSITY  
SCHOOL OF MEDICINE

Thesis

**PARIETAL CELL DISTRIBUTION INFORMS  
GASTRIC BYPASS PROCEDURE**

by

**NADIA A. RUKAVINA**

BMSc, University of Western Ontario, 2020

Submitted in partial fulfillment of the  
requirements for the degree of  
Master of Science

2022

© 2022 by  
NADIA A. RUKAVINA  
All rights reserved

Approved by

First Reader

---

Jonathan J. Wisco, Ph.D.  
Associate Professor of Anatomy and Neurobiology

Second Reader

---

Linda Afifi, Ph.D.  
Assistant Professor of Anatomy and Neurobiology

## **DEDICATION**

I would like to dedicate this work to my parents, Elizabeth and Steven. Thank you for  
your unwavering support.

## **ACKNOWLEDGMENTS**

I would like to acknowledge those who generously donated their body to Boston University School of Medicine, for the advancement of education and research. Thank you for your gift.

I would also like to acknowledge my mentor, Dr. Jonathan Wisco. Thank you for your guidance and your patience.

# **PARIETAL CELL DISTRIBUTION INFORMS GASTRIC BYPASS**

## **PROCEDURE**

**NADIA A. RUKAVINA**

### **ABSTRACT**

Introduction: Roux-en-Y Gastric Bypass (RYGB) is a common bariatric procedure that facilitates weight loss and reduces co-morbidities of obesity. A common complication is marginal ulceration, caused by an overproduction of hydrochloric acid from the gastric pouch, and acid insult to the unprotected jejunal mucosa. The exact distribution of parietal cells in the stomach is not agreed upon. We hypothesize that there are regions of low density of parietal cells, and that these areas can allude to the optimal dimensions of the gastric pouch to reduce acid production.

Methods: Seventeen cadaveric subjects were used in this study. A standardized schematic based on anatomical landmarks was created to examine nine operationally defined stomach segments of the cardiac and fundic stomach. Punch biopsies from the center of each of the stomach segments were collected and subsequently analyzed using immunohistochemistry. Sections were stained with Hydrogen Potassium ATPase Beta monoclonal antibody. Computational analysis was used to calculate the number of parietal nuclei per ROI area ( $\mu\text{m}^2$ ). Chi-Square Goodness of Fit analysis was performed to determine if there is a difference in parietal cell density between segments.

Results: Amongst all different stomach segments, the number of parietal nuclei per ROI area ( $\mu\text{m}^2$ ) is significantly different across all sections from the expected value of all sections being equal  $X^2(8)=21.82, p=0.005$ . Trends in the data illustrated that the distal lesser curvature contains a high concentration of parietal cells.

Conclusion: The analysis demonstrates that there is a difference in parietal cell density between various stomach segments, with some segments illustrating lower parietal cell density. These findings inform our recommendation of a horizontal gastric pouch, to include the proximal cardia and fundus adjacent to the gastroesophageal junction, in order to minimize the density of parietal cells in the gastric pouch and reduce the incidence of marginal ulceration following RYGB.

## TABLE OF CONTENTS

DEDICATION .....	iv
ACKNOWLEDGMENTS .....	v
ABSTRACT.....	vi
TABLE OF CONTENTS.....	viii
LIST OF TABLES .....	x
LIST OF FIGURES .....	xi
LIST OF ABBREVIATIONS.....	xii
INTRODUCTION .....	1
METHODS .....	6
Subjects .....	6
Tissue Collection .....	6
Histological Analysis .....	11
Computational Analysis.....	12
Manual Cell Counting.....	14
Statistical Analysis.....	15
RESULTS .....	16
Demographics .....	16
Epithelial Tissue Types.....	16
Manual Cell Counting.....	18
Chi-Square Results .....	19
DISCUSSION.....	23

Future Directions .....	32
Strengths and Weaknesses .....	33
BIBLIOGRAPHY.....	34
CURRICULUM VITAE.....	36

## LIST OF TABLES

Table 1. Summary of Samples Collected.....	16
Table 2. Descriptive Statistics.....	20

## LIST OF FIGURES

Figure 1. Gastric bypass surgery.....	2
Figure 2. Schematic of stomach using anatomical landmarks .....	7
Figure 3. Biopsies for regions of interest.....	9
Figure 4. Schematic on cadaveric stomach.....	10
Figure 5. Computational analysis versus manual cell counting.....	14
Figure 6. Representative images of epithelium types .....	18
Figure 7. Median number of parietal nuclei per ROI area for each stomach segment .....	21
Figure 8. Histological sections from each segment of interest .....	22
Figure 9. Heat map; likelihood of parietal cells.....	26
Figure 10. Heat map; normalized parietal nuclei counts .....	26
Figure 11. Recommended gastric pouch; schematic.....	29
Figure 12. Recommended gastric pouch; cadaveric stomach.....	30

## LIST OF ABBREVIATIONS

BUSM	Boston University School of Medicine
GEJ	Gastroesophageal junction
GERD	Gastro-esophageal reflux disease
H+/K+	Hydrogen Potassium
IHC	Immunohistochemistry
ROI	Region of Interest
RYGB	Roux-en-Y Gastric Bypass
SC	Simple Columnar
SSNK	Stratified Squamous Non-Keratinized
$\mu\text{m}$	Micrometer ( $1 \times 10^{-6}$ meters)

## INTRODUCTION

Roux-en-Y gastric bypass (RYGB) is a common type of bariatric surgery, performed for the purpose of weight loss in obese patients, in an attempt to reduce the comorbidities associated with obesity<sup>1</sup>. Comorbidities of obesity include hypertension, hyperlipidemia, diabetes and obstructive sleep apnea<sup>2</sup>. Gastric bypass surgery is reported to improve or completely resolve such comorbidities<sup>2</sup>, and extend the life expectancy of obese patients.

The gastric bypass procedure involves the creation of a small gastric pouch from the larger stomach. A gastro-jejunostomy is then performed, where in this new smaller pouch is connected to a more distal portion of the small intestine, the jejunum<sup>3</sup>. With this altered anatomy, when food is consumed, it bypasses a large portion of the stomach and the duodenum, effectively limiting food absorption<sup>3</sup>, making this procedure *malabsorptive*. Additionally, this gastric pouch is only able to hold about 1 oz of food, as compared to a normal adult stomach which can expand to hold up to 32 oz. Thus, this procedure limits food intake, making it *restrictive*. The combination of malabsorptive and restrictive aspects of this procedure makes it effective for facilitating weight loss in obese patients.

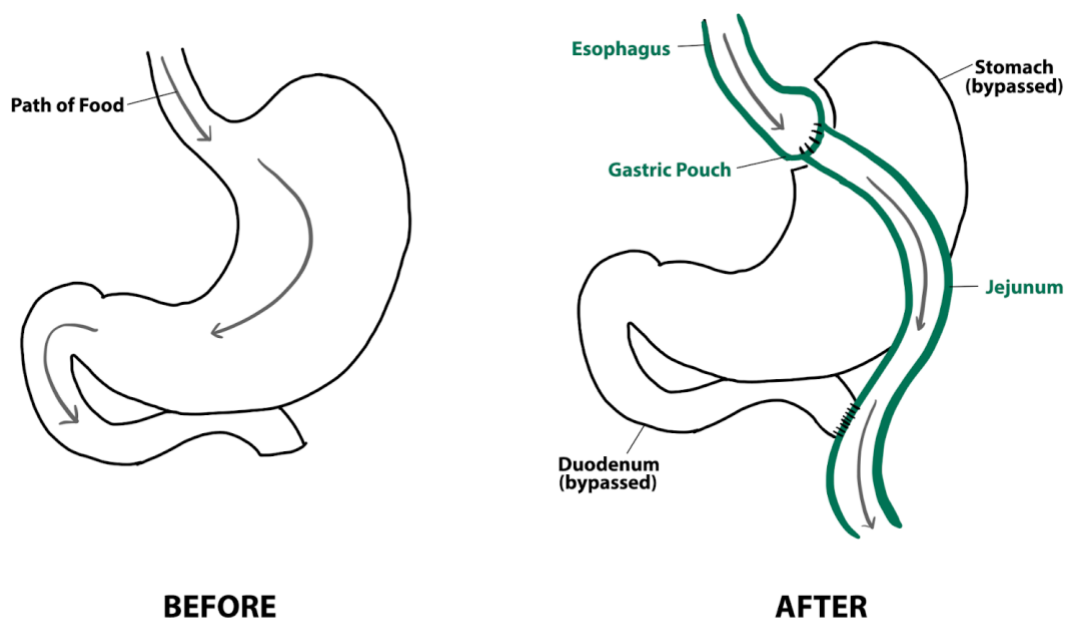


**Figure 1. Normal anatomy (left); food travels through the alimentary canal. Gastric bypass procedure (right). A small gastric pouch is created distal to the gastroesophageal junction (GEJ). A gastro-jejunostomy is performed, connecting the jejunum to the pouch. The Roux limb is made by anastomosis of the duodenum to the distal jejunum. Food travels through altered anatomy, bypassing a large portion of the stomach, and the duodenum.**

While RYGB has many benefits for obese patients, a common complication is marginal ulceration. This occurs in 1-16% of patients who undergo this surgery<sup>3</sup>, although the symptoms are often confused with other postoperative complaints such as epigastric pain<sup>4</sup>, so the incidence is likely even higher. Marginal ulcers occur at the gastro-jejunal anastomosis and are thought to be caused by peptic digestion of the

unprotected jejunal mucosa, enhanced by acid produced in the gastric pouch<sup>3</sup>. In normal digestion, the duodenum has innate buffering capabilities. Duodenal epithelium secretes bicarbonate to neutralize acid from the stomach and protect the duodenum from autodigestion by pepsin in active gastric juice<sup>5</sup>. But, following the gastro-jejunostomy in a gastric bypass procedure, the jejunum is exposed to stomach contents that it does not have protection against, thus its mucosa is susceptible to injury and ulceration.

Conventionally, there are different types of mucosa throughout the stomach. Cardiac mucosa is characterized by mucus-secreting cells, and this region contains little to no parietal cells<sup>6</sup>. Corpus (body) mucosa is anatomically defined as the body and fundus of the stomach, and it contains numerous parietal cells and chief cells<sup>6</sup>, which secrete hydrochloric acid and pepsinogen/gastric lipase, respectively. Antral mucosa contains mucus-secreting cells, similar to the cardiac mucosa region, and G-cells which produce gastrin<sup>6</sup>.

Typically, the gastric pouch is created by using the cardia of the stomach, for multiple reasons. First, the cardia contains longitudinal, circular and oblique muscle fibers, making this area strong and resistant to stretching<sup>7</sup>. Secondly, this region is thought to have minimal parietal cell distribution, thus reducing the amount of gastric acid the pouch is able to make. This being said, it is not fully known (or agreed upon) where the boundaries for cardiac mucosa are. Some studies have suggested that this mucosa is only present as a small band of a few millimeters around the gastro-esophageal junction<sup>6</sup> – this area could be denoted as the ‘*true cardia*’. As such, many gastric pouches extend into the proximal lesser curvature of the stomach. Extending the pouch vertically

into the lesser curvature as opposed to horizontally into the fundus is beneficial because the fundus is elastic by nature and may dilate significantly over time<sup>7</sup>, defeating the purpose of the small gastric pouch to facilitate weight loss. Although, studies have reported that the lesser curvature of the stomach actually contains a high concentration of parietal cells, which increases the ability for the gastric pouch to produce acid,<sup>7</sup> thus contributing to marginal ulcerations.

Typical dimensions for the gastric pouch are about 4x5cm, using the left gastric artery and vein as an anatomical landmark, as well as the cardiac notch<sup>8</sup>. This being said, there is no general consensus for the exact size of the gastric pouch. Larger pouch size and orientation has been seen to predispose patients to marginal ulceration following this procedure<sup>4</sup>. Thus, it is thought that by constructing a tiny pouch close to the gastro-esophageal junction (approximately 2x3cm) the relative amount of non-acid producing cardiac mucosa can be increased, and the number of acid-producing parietal cells can be decreased<sup>6</sup>. But, it is very difficult to construct a gastric pouch with predominantly non-acid producing cardiac mucosa, because we do not know the exact margins of the *cardia*. While it is thought that parietal cells are highly distributed in the body and fundus regions of the stomach, we do not know the exact distribution of these acid-producing cells. Further investigation into the parietal cell distribution of the stomach would provide important insight into areas to *avoid* when constructing the gastric pouch, and could inform surgeons of more exact dimensions to use when constructing the gastric pouch in order to reduce the complication of marginal ulceration.

The *aim* of the present study is to investigate the parietal cell distribution in the stomach to provide insight on the optimal size and location of the gastric pouch to be made during gastric bypass surgery, according to standardized anatomical landmarks. Limiting the density of parietal cells in the gastric pouch will minimize the amount of gastric acid that the pouch is able to produce, thus mitigating the incidence of marginal ulceration following this procedure. We *hypothesize* that there are areas of low distribution of parietal cells in the stomach, and once these regions have been identified, as defined by standardized anatomical landmarks, they will allude to the optimal dimensions and location of the gastric pouch in any given subject.

## **METHODS**

### **Subjects**

This study included 17 cadaveric subjects from Boston University School of Medicine; 10 males and 7 females. Information about the embalming process was obtained from the Department of Anatomy and Neurobiology at BUSM. The cadaveric subjects were flushed with a combination of distilled water and Primol solution (Hydrol Chemical). Then, the subjects were perfused with Cornell Embalming Solution. Once perfused, the subject is allowed to sit for 8 weeks, so as to allow the tissue to completely permeate. Tissue biopsies were collected about one year after embalming.

### **Tissue Collection**

We first created a standardized schematic of the stomach, using branches of the left gastric artery, and right gastroepiploic artery, as well as other features of the stomach, such as the cardiac notch and pylorus, as anatomical landmarks from which to draw the standard grid lines onto the stomach (Figure 2).

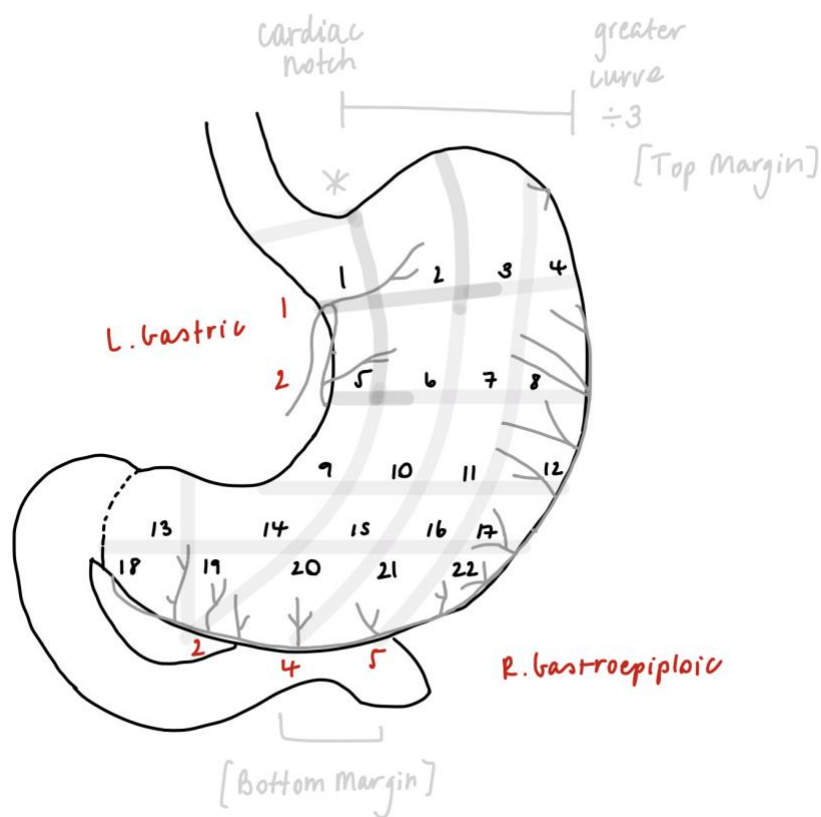


**Figure 2. A schematic of the stomach using anatomical landmarks. Horizontal grid lines were drawn using branches of the left gastric artery, and the pyloric sphincter. Vertical grid lines were drawn using the cardiac notch, equal distance to the greater curvature, and branches of the right gastroepiploic artery. Segments were number 1 through 22, on the anterior and posterior side of the stomach.**

Each segment was numbered, 1 through 22, on the anterior (denoted as ‘A’) and posterior (denoted as ‘P’) side of the stomach. Segments 1 and 5 each had subsections A–D, for a total of 56 sections per stomach.

The stomach from each donor was revealed *in situ*. The left gastric artery and right gastroepiploic artery were delineated, so that branches could be clearly identified. The stomach was removed from the abdomen through standardized cuts to the esophagus at approximately 2 cm proximal to the gastro-esophageal junction through palpation, and the duodenum at approximately 2 cm distal to the pyloric sphincter through palpation. Once removed, grid lines were drawn onto the stomach with black marker using a ruler, guided by the previously drawn schematic and anatomical landmarks on individual stomachs.

The location of the *horizontal gridlines* were defined as follows: 1st branch of left gastric artery, 2nd branch of the left gastric artery, the top of the pyloric sphincter (angle incisura), and either i) the midpoint of the pyloric sphincter or ii) the bottom of the pyloric sphincter, depending on the individual variation of the stomach shape and size.

The location of the *vertical gridlines* were defined as follows: the first line was from the cardiac notch to 2nd branch of the right gastroepiploic artery, running parallel to the lesser curvature. Then, the distance from the cardiac notch to the greater curvature of the stomach was measured with a ruler and divided into three sections. The second line was from  $\frac{1}{3}$  distance of the cardiac notch to the greater curvature, down to the 4th branch of the right gastroepiploic artery. The third line was from  $\frac{2}{3}$  distance of the cardiac notch to the greater curvature, down to the 5th branch of the right gastroepiploic artery. The final vertical line was from the 2nd branch of the right gastroepiploic artery, straight upwards through the pylorus region (to create sections 13 and 18).

The schematic with labelled numbered sections was used for reference while creating these gridlines on individual stomachs. Finally, for sections 1 and 5, an 'X' shape was drawn through the square, to create subsections A/B/C/D (starting from the left, moving clockwise). (Figure 3).

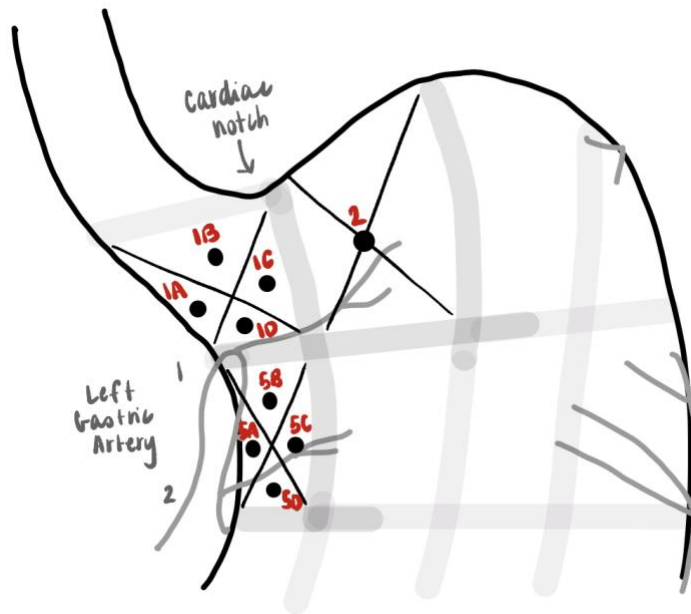


**Figure 3. Biopsies for regions of interest. An 'X' shape was drawn through segments 1 and 5, to create subsections A, B, C, and D, on both anterior and posterior sides. Biopsies were taken from the midpoint of each section or subsection.**

A 4 mm biopsy punch was used. One biopsy was taken from the middle of each section, on the anterior and posterior sides of the stomach. To take the biopsy from the posterior side, we went through the anterior side hole, through to the posterior side, so

that the schematic only needed to be drawn on the anterior side. Once removed, the biopsies were cut in half, placed in micromesh cassettes and stored in formalin.



**Figure 4. The schematic of the stomach according to anatomical landmarks applied to a cadaveric stomach. 4mm punch biopsies were taken from the middle of each segment.**

When creating the schematic for the stomach, particular anatomical landmarks were used due to adherence to current clinical practice. Currently, anatomical landmarks for making the gastric pouch during gastric bypass surgery utilize the 2nd branch of the left gastric artery as the horizontal dimension, and the cardiac notch as the vertical dimension<sup>8</sup>. Thus, we started with these landmarks to create our schematic. Additionally,

it has been suggested that the 2nd branch of the right gastroepiploic artery be used as a vertical landmark for a gastric sleeve procedure<sup>2</sup>, where the sleeve runs from this anatomic landmark to the cardiac notch, so we incorporated this dimension into our schematic, illustrated as the first vertical grid line.

We used the typical pouch size as our area of interest for this study, and focused on these segments to investigate parietal cell distribution. These subdivided regions allowed us to capture higher resolution biopsies that would correspond to different pouch sizes. Biopsies from sections 1 (A/B/C/D), 2, and 5 (A/B/C/D), from the anterior side of the stomach, were used for analysis, for a total of 9 sections per subject.

### **Histological Analysis**

The biopsies were sent for immunohistochemical processing to iHisto (Salem, MA). Biopsies were paraffin-embedded, and incubated with a H<sup>+</sup>/K<sup>+</sup> ATPase Beta monoclonal primary antibody, Clone 2G11 (Novus Biologicals, Catalog #NB300-583) at 1:1000 dilution. A secondary antibody tagged with a 3,3'-Diaminobenzidine (DAB) chromogen kit (ImmPRESS® HRP Horse Anti-Rabbit IgG PLUS Polymer Kit, Peroxidase, Vector Laboratories, Catalog #MP-7801) then reacted with the primary antibody. Sections were counterstained with hematoxylin. Stained sections were scanned using to create 40x virtual microscopy images.

For each biopsy, series of images captured at 30x using QuPath (<https://qupath.readthedocs.io/en/stable/>) were assembled into a montage, correcting for image distortion and lens flare, using Adobe Photoshop CS (Adobe, Inc., San Jose, CA). Regions of interest (ROI) corresponding to the epithelium of the biopsies were segmented

in Photoshop. These ROIs served as the template for an automated set of Python code used to process these images for DAB positive pixel segmentation and count normalized to the area of ROI.

### **Computational Analysis**

The glob module in Python

(<https://github.com/python/cpython/blob/3.10/Lib/glob.py>) was used to extract the image paths and names of these raw and highlighted images. Lists containing these strings were sorted alphabetically and used as an order guide for the subsequent image processing algorithms to ensure that raw and highlighted images of the same index corresponded.

Images containing blue highlighted regions of interest (ROIs) were filtered to display pixels with red values below 150 on a 255 scale, green pixels with values below 100, and blue pixels with values above 110. This process isolated the blue color that was used to annotate/highlight the ROI in these images. These filtered images were converted from RGB to grayscale, and Otsu's<sup>10</sup> method for thresholding from the Scikit-image library<sup>11</sup> was used to binarize the ROI. This method maximizes the variance between two classes of pixels, the ROI and background, within our study, effectively minimizing the intra-class variance. The ROIs were assigned pixel values of 1, and the background pixels were assigned values of 0. Objects smaller than 0.5% of the total area of the image were removed from the image to further isolate the ROI. The sum of pixels equal to 1 in the binary images was recorded as the area of the ROI.

Since the microscopy images had inconsistent staining, an adaptive threshold was needed to isolate parietal nuclei that varied in intensity from image to image. The mean

value of pixels in the red, green, and blue channels of the image were computed. The number of white pixels in the whole image was also calculated. Using the color channel mean values and the number of white pixels, mean red, green, and blue pixel values were obtained that excluded white pixels to be more accurate. The raw images were filtered to only contain pixels with red channel values smaller than about 0.96% of the red mean excluding white pixels, green channel values greater values than about 0.49% of the green mean excluding white pixels, and blue channel values smaller values than about 0.76% of the red mean excluding white pixels. This adaptive thresholding method was used to isolate all of the parietal nuclei in the raw images. The resulting images were converted from RGB to grayscale and binarized using Li<sup>12</sup> thresholding from the Scikit-image library.<sup>11</sup>

The pixels that met our color channel thresholds, ideally parietal nuclei, were assigned pixel values of 1, and all other pixels were assigned values of 0. Objects smaller than 5 pixels were filtered out of this binary image. The resulting nuclei in the image are then “closed,” using a neighborhood (as measured by Euclidean distance) of a 3 pixel radius. This consists of dilation followed by erosion using the closing function in Scikit-image to close outlines of nuclei that were not quite connected. All nuclei were then filled using the “reconstruction” function in Scikit-image. The arrays of these resulting images which include segmented parietal nuclei, were multiplied by the corresponding arrays of the binary ROI images to output images that contained the total parietal nuclei within the defined ROI. The image was labeled using Scikit-image library’s labeling tool, which outputs a “Labeled array, where all connected regions are assigned the same integer

value.”<sup>11</sup> In this image, each nucleus was labeled and a new image was created, highlighting the bounding box of nuclei of areas between 5 and 100 pixels and eccentricities below 0.8 in a red bounding box. Counts of the number of cells that met these criteria were also obtained. The image with highlighted cells was used for visual validation of the nucleus counts. A Pandas data frame was used to organize data.

### Manual Cell Counting

For some of the histological slides, there was not enough hematoxylin counter stain; the algorithm was not visually accurate according to the anatomy. Thus, following the automated cell counting through computational analysis, manual cell counting was performed to verify cell counts on such slides that visually appeared to illustrate aberrant parietal nuclei counts. Histological slides were viewed with QuPath. The grid feature and point tool were used to count number of parietal nuclei in each grid square, and numbers were summed at the end. Manual cell counting of parietal nuclei was completed twice for each histological slide.

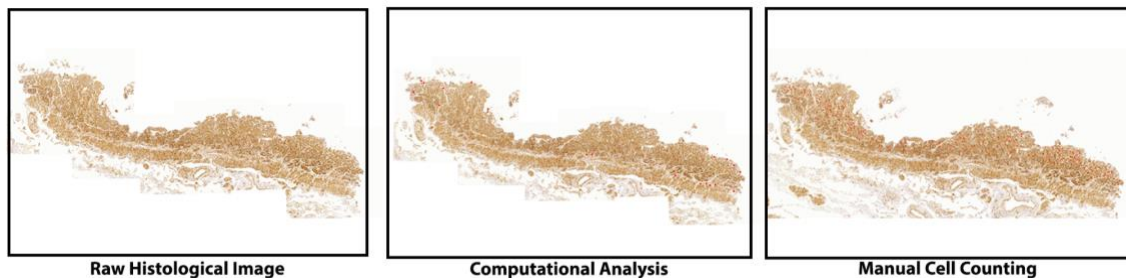


**Figure 5. Raw histological slide of subject with not enough hematoxylin stain (left panel). Computational analysis of slide (middle panel). Manual cell counting of slide (right panel). Red dots indicate parietal nuclei counts.**

## Statistical Analysis

Each cadaveric biopsy (cadaveric subject, stomach segment) was considered to be a separate subject.

The median normalized number of nuclei per ROI area was transformed through multiplication by a factor of  $10^5$  to fulfill an assumption of the Chi-Square Goodness of Fit test; expected frequencies in each group of a categorical variable must be equal to at least 5 (Laerd Statistics). This transformation allowed for the data to be described in whole numbers, making them in an acceptable range to meet the criteria to run the Chi-Square Goodness of Fit analysis through SPSS.

Results were analyzed through descriptive statistics and Chi-Square Goodness of Fit test using SPSS. Statistical significance was set at  $\alpha=0.05$ .

## RESULTS

### Demographics

There were 17 cadaveric subjects included in this study; 10 males, and 7 females. From each cadaveric subject, nine stomach biopsies were sent for analysis, for a total of 153 samples.

### Epithelial Tissue Types

The epithelial architecture of some of these samples did not remain intact, thus these samples were not able to be analyzed. Samples with epithelial architecture that were intact included simple columnar (SC) epithelium and stratified squamous non-keratinized (SSNK) epithelium. SSNK epithelium contains no gastric glands, and thus no parietal cells, so these samples were counted as 0 parietal nuclei/ROI area ( $\mu\text{m}^2$ ).

**Table 1. Total samples collected from regions of high interest of 17 cadaveric subjects. SC indicates simple columnar epithelium, SSNK indicates stratified squamous non-keratinized epithelium, and were analyzed for parietal cells. (–) indicates epithelial architecture of the sample was not intact and not able to be analyzed.**

	1AA	1AB	1AC	1AD	2A	5AA	5AB	5AC	5AD
1	–	–	–	–	SC	–	–	SC	SC
2	SSNK	SSNK	–	–	SSNK	SC	SC	–	–
3	–	SSNK	–	–	–	–	–	–	–

4	-	-	-	-	-	SSNK	-	-	-
5	-	SSNK	-	-	-	-	-	-	-
6	-	-	-	-	-	-	-	-	-
7	-	SC	-	-	-	SSNK	-	SC	-
8	SSNK	SSNK	-	-	-	-	-	-	-
9	SC	SC	SC	SC	SC	SC	SC	-	SC
10	-	-	-	-	-	-	-	-	-
11	SC	-	SC	SC	-	SC	SC	SC	SC
12	-	-	-	-	SSNK	-	-	-	-
13	-	SC	-	-	-	-	SC	-	SC
14	SC	SC	-	SC	SSNK	-	SC	SC	SC
15	-	SC	-	SC	SC	SC	SC	SC	SC
16	-	-	SC	SC	-	-	-	-	-
17	SC	-	-	SC	-	-	SC	-	SC

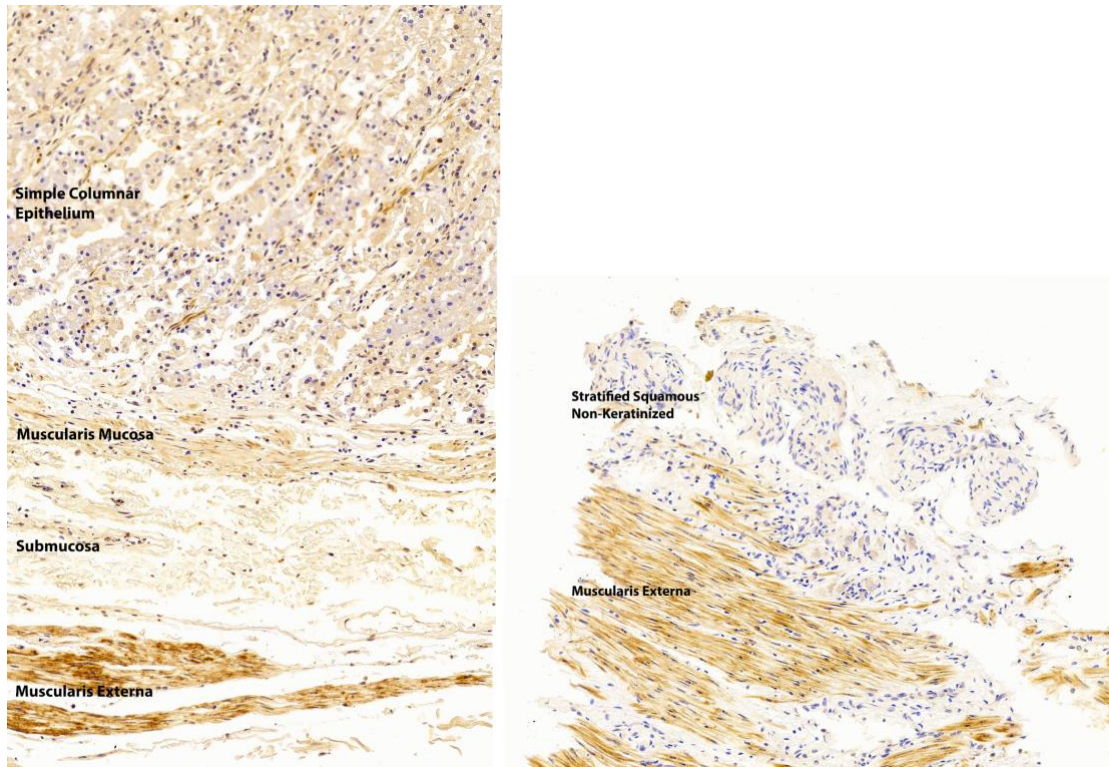


**Figure 6. Representative image of simple columnar epithelium (left) and stratified squamous non-keratinized epithelium (right). Both images are from section 2A.**

**(IHC)**

### **Manual Cell Counts**

A paired t-test was performed to verify that the two trials of manual cell counting in QuPath obtained the same cell count [ $t(5)=0.601$ ,  $p=0.574$ ]. There was no statistical difference between the two trials; an average of the two trials was used. The manual cell count replaced the computational counts for six slides, and the values were used to calculate the normalized parietal nuclei per ROI area.

## Chi-Square Results

Due to the small sample size, and unequal numbers of biopsies per stomach segment, the normalized parietal nuclei counts are not normally distributed; thus, the *median* density of parietal cells was reported.

Section 1AA samples included 2 stratified squamous non-keratinized (SSNK) epithelium (= 0) and 4 simple columnar (SC) epithelium; Section 1AA had a median of  $1.32 \times 10^{-4}$  parietal nuclei/ROI area ( $\mu\text{m}^2$ ) (SD= $1.14 \times 10^{-4}$ ). Section 1AB samples included 4 SSNK epithelium (=0) and 5 SC epithelium; Section 1AB had a median of  $1.49 \times 10^{-4}$  parietal nuclei /ROI area ( $\mu\text{m}^2$ ) (SD= $1.34 \times 10^{-4}$ ). Section 1AC samples included 4 SC epithelium; Section 1AC had a median of  $1.56 \times 10^{-4}$  parietal nuclei/ROI area ( $\mu\text{m}^2$ ) (SD= $4.61 \times 10^{-5}$ ). Section 1AD samples included 6 SC epithelium; Section 1AD had a median of  $2.42 \times 10^{-4}$  parietal nuclei/ROI area ( $\mu\text{m}^2$ ) (SD= $1.07 \times 10^{-4}$ ). Section 2A samples included 3 SSNK epithelium (=0) and 3 SC epithelium; Section 2A had a median of  $1.66 \times 10^{-5}$  parietal nuclei/ROI area ( $\mu\text{m}^2$ ) (SD= $9.99 \times 10^{-5}$ ). Section 5AA samples included 2 SSNK epithelium and 4 SC epithelium. Section 5AA had  $8.82 \times 10^{-5}$  parietal nuclei/ROI area ( $\mu\text{m}^2$ ) (SD= $1.08 \times 10^{-4}$ ). Section 5AB samples included 7 SC epithelium; Section 5AB had a mean of  $1.88 \times 10^{-4}$  parietal nuclei/ROI area ( $\mu\text{m}^2$ ) (SD= $1.06 \times 10^{-4}$ ). Section 5AC samples included 5 SC epithelium; Section 5AC had a mean of  $1.84 \times 10^{-4}$  parietal nuclei/ROI area ( $\mu\text{m}^2$ ) (SD= $8.31 \times 10^{-5}$ ). Section 5AD samples included 7 SC epithelium; Section 5AD had a mean of  $1.81 \times 10^{-4}$  parietal nuclei/ROI area ( $\mu\text{m}^2$ ) (SD= $9.41 \times 10^{-5}$ ).

**Table 2. Descriptive statistics for each stomach segment. Normalized nucleus count is defined as number of parietal nuclei per ROI area ( $\mu\text{m}^2$ ). All values are expressed to the power of  $10^{-4}$ .**

<u>Stomach Segment</u>	<u>Median Normalized Nucleus Count</u>	<u>SD</u>
1AA	1.32	1.14
1AB	1.49	1.34
1AC	1.57	0.461
1AD	2.42	1.07
2A	0.166	0.999
5AA	0.882	1.08
5AB	1.88	1.06
5AC	1.84	0.831
5AD	1.81	0.941

A Chi-Square Goodness of Fit test was performed to determine whether the proportion of normalized parietal nuclei per ROI area was equal between the nine stomach segments. The proportions *did* differ by stomach segment,  $X^2(8) = 21.82$ ,  $p=0.005$ .

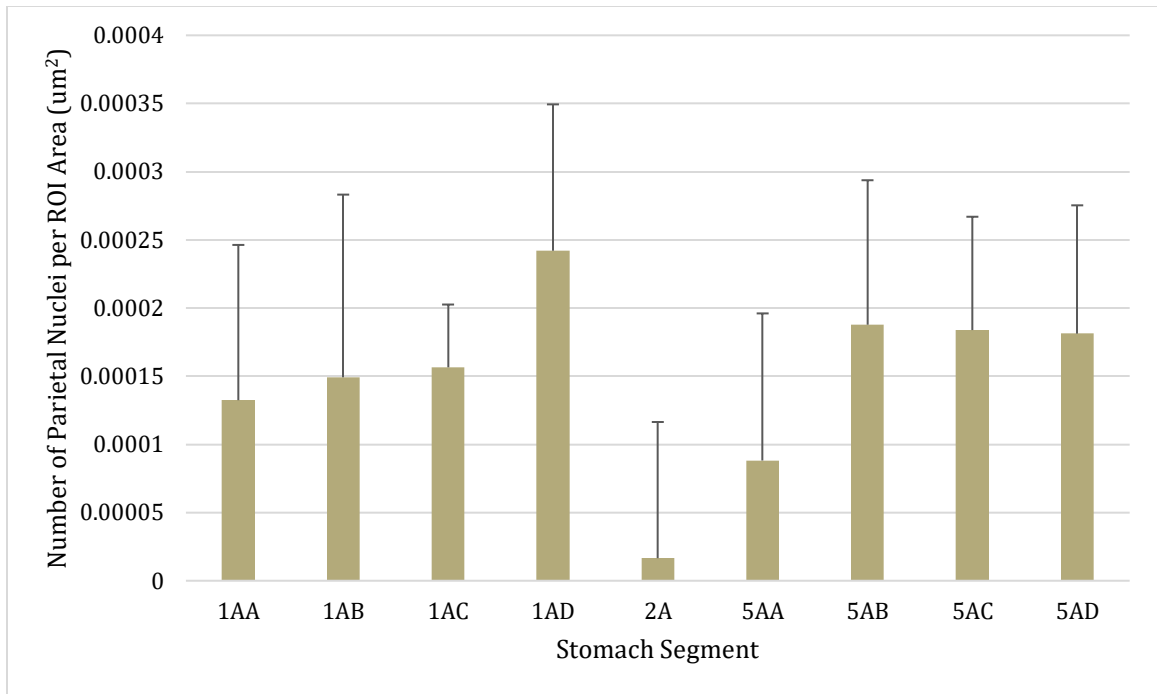


**Figure 7. Median (+/- SD) number of parietal nuclei per ROI area ( $\mu\text{m}^2$ ) (normalized nucleus count) for each stomach segment. ( $p=0.05$ ). Proportion of normalized parietal nuclei differed between the nine stomach segments ( $p=0.005$ ).**

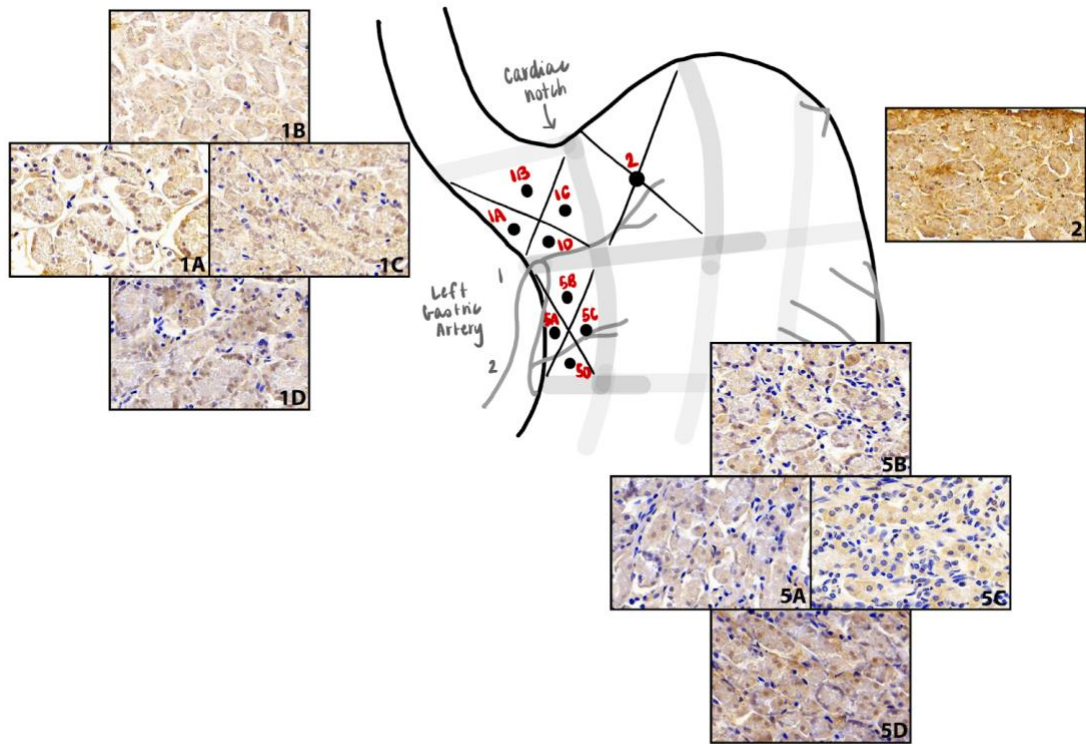


**Figure 8. Histological sections from each segment of interest. All sections were taken from the same subject #9, with the exception of section 5C, taken from subject #14.**

## DISCUSSION

Gastric bypass is one of the most common bariatric surgeries, because this method is both restrictive and malabsorptive. Restrictive, because the small physical size of the gastric pouch restricts caloric intake. Malabsorptive, because by bypassing the duodenum, there is a lack of chemical breakdown of the food you are able to consume, thus less food is absorbed by the body. Another popular alternative is the *sleeve gastrectomy*. This method involves stapling the stomach approximately from the cardiac notch down to the 2nd branch of the right gastroepiploic artery,<sup>2</sup> removing the majority of the body and fundus of the stomach, leaving behind a small tube-like stomach, and leaving the duodenum untouched. Although, these anatomical landmarks are not standardized; gastric sleeve size/shape may differ between individuals leading to inconsistencies in reported weight loss<sup>13</sup>. This procedure may not result in as effective weight loss compared to gastric bypass, because a much larger portion of the stomach is left behind, so there is not as much of a restriction on food intake. Additionally, due to the duodenum being left intact, there is no malabsorptive aspect of this procedure, and food will continue to be absorbed normally. A benefit of sleeve gastrectomy is that this method does not see marginal ulcerations because normal anatomy is maintained; the duodenum has innate buffering capabilities and can withstand the gastric acid still being produced by the remaining stomach.

In an attempt to reduce the incidence of marginal ulcerations that occur following gastric bypass procedure, we aimed to explore the distribution of parietal cells, specifically in the region of interest where a typical gastric pouch is located. Limiting the

number of parietal cells in the region of interest would reduce the amount of gastric acid the pouch is able to produce, and limit the acid insult on the jejunum following the gastrojejunostomy.

In a gastric bypass procedure, the gastric pouch is made from the gastric *cardia*, anatomically described as the region just distal to the gastroesophageal junction (GEJ), and histologically defined as containing mucous glands with only mucus-secreting cells<sup>14</sup>. But the exact size and location of this region has long been up for debate. Some studies report that this region extends 10 to 30mm distal to the GEJ<sup>14</sup>, others report that the region is even smaller. Stomach size and shape varies from person to person, thus it can be difficult, if not impossible, to determine an exact length or width of the *cardia* region that can be applied to all individuals. Instead, using anatomical landmarks that are quite standard between individuals, and analyzing the histology of these predetermined regions, is perhaps a better way to describe this area of the stomach. This would allow surgeons to use anatomical landmarks that define the boundaries of the gastric cardia as a guide to making the gastric pouch the same way every time.

Currently, a typical gastric pouch has the approximate anatomical landmarks of the cardiac notch as the vertical dimension, and the second branch of the left gastric artery as the horizontal dimension. In our schematic, this region is illustrated by Segment 1 and Segment 5. We also explored Segment 2 in our region of interest, as this area is directly adjacent to a typical gastric pouch. Basing the gastric pouch dimensions on arterial landmarks is ideal because it provides a standardized landmark in any given subject, but perhaps more importantly, it ensures that the pouch is getting a good blood

supply; the left gastric artery has ample blood pressure to ensure the new gastric pouch is well nourished and reduce the risk of ischemia.

Chi-Square Goodness of Fit test was performed to determine whether the proportion of normalized parietal nuclei per ROI area was equal between the nine segments (denoted as 'expected' value). The proportions did differ by stomach segment,  $X^2(8) = 21.82, p = 0.005$ . Amongst all different sections, it was shown that the number of parietal cells per ROI area ( $\mu\text{m}^2$ ) is significantly different across all sections, from the expected value of all sections being equal.

Due to a small sample size, statistical tests to determine which segments specifically are different from one another were not able to be conducted. However, patterns from the data show that there are generally fewer parietal nuclei in segment 2, and proximal segment 1 (1A, 1B, 1C), areas that are just adjacent to the gastroesophageal junction (Table 2, Figure 10). These same trends are apparent through visual analysis of histological images (Figure 8).

The majority of the gastrointestinal tract, including the stomach, is characterized by having simple columnar (SC) epithelium, whereas the esophagus is characterized by stratified squamous non-keratinizing (SSNK) epithelium. Interestingly, SSNK epithelium was found in segments along the lesser curvature (1A, 5A), the proximal fundus (2) and just distal to the gastro-esophageal junction (1B). Parietal cell counts in samples composed of SSNK epithelium were considered to equal 0.

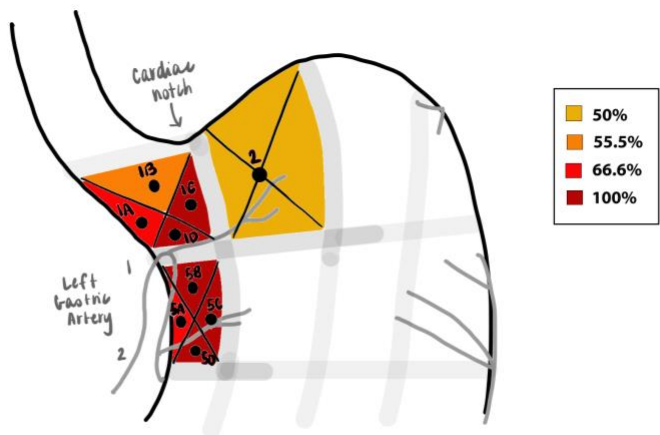


**Figure 9. Data driven heat map of the percentage of sections that contain parietal cells. Yellow regions contain parietal cells 50% of the time. Orange regions contain parietal cells 55.5% of the time. Red, 66.6% of the time, and dark red, 100% of the time.**

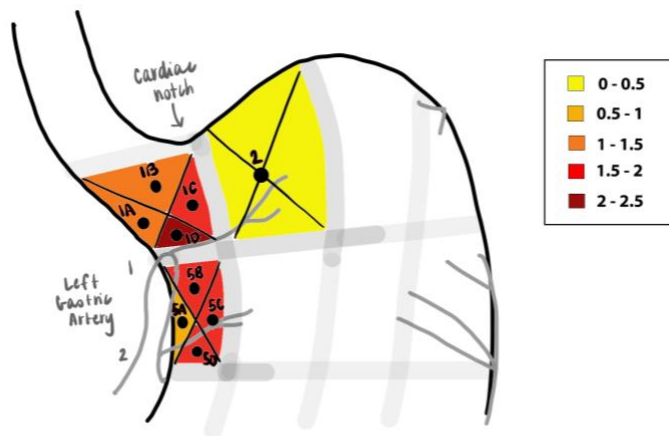


**Figure 10. Data driven heat map of the median normalized number of parietal nuclei per ROI area ( $\mu\text{m}^2$ ), all values are expressed to the power of  $10^{-4}$ . Yellow**

**regions, 0 – 0.5. Light orange regions 0.5 – 1. Dark orange regions 1 – 1.5. Red regions 1.5 – 2. Dark red regions, 2 – 2.5.**

Stojacic et al<sup>14</sup> described the cardia as a ‘transition zone’ from the stratified squamous epithelium of the esophagus, to the oxyntic glands of the body of the stomach. In this transition zone, there are various types of mucosa, which were noted in our experiment. “Pure cardiac-type” mucosa describes the stereotypical cardiac mucosa, containing mucous glands with *only* mucus-secreting cells.<sup>14</sup> “Oxyntocardiac-type mucosa” describes mucous glands with mainly mucus-secreting cells, and some sporadic parietal cells.<sup>14</sup> “Oxyntic-type mucosa” describes typical gastric glands, containing many parietal and chief cells.<sup>14</sup> From our findings, it could be said that our segments represent oxyntocardiac-type mucosa and oxyntic-type mucosa, but we did not find any pure cardiac-type mucosa.

It has also been noted that histologically, cardiac mucosa extends as a band no more than 10mm around the gastro-esophageal junction.<sup>14</sup> Our findings support this notion. Section 1B is on the margin of the gastro-esophageal junction, yet this region still contained an invariable amount of parietal cells. Thus, it is reasonable to conclude that the ‘true’ cardia does not extend very far past the esophagus.

Histologically, the ‘true cardia’ is far too small to use to make a gastric pouch. Based on general trends of parietal cell distribution between segments, and likelihood to encounter SSNK epithelium, thus containing no parietal cells, the gastric pouch should ideally contain Section 1 and Section 2.

Given the results of the Chi-Square Goodness of Fit test, that normalized parietal nuclei counts are significantly different across all nine stomach sections, from the expected value of all sections being equal, we can reject the null hypothesis, and accept the alternative hypothesis. We can conclude that there is a difference in the density of parietal cells among different stomach segments, and that there are areas of low distribution of parietal cells in the stomach. Such findings allude to the optimal dimensions and location of the gastric pouch in any given subject.

General trends of normalized parietal nuclei in each segment suggest that section 2, and proximal section 1 (1A, 1B, 1C) have lower normalized parietal nuclei counts, compared to more distal regions (1D, section 5). This finding, coupled with the common finding of SSNK epithelium in certain stomach regions (1A, 1B, 2, 5A), meaning that parietal nuclei count equals 0, led us to our conclusion for our recommendation on the optimal size and location of the gastric pouch.

These findings were based on the assumption that all subjects' stomach health was normal. If a patient had chronic gastro-esophageal reflux disease (GERD), one would expect the number of parietal cells in segments 1 and 2 to increase as a result of esophageal metaplasia, where columnar epithelium replaces the SSNK epithelium of the esophagus as a result of prolonged acid injury.<sup>15</sup>

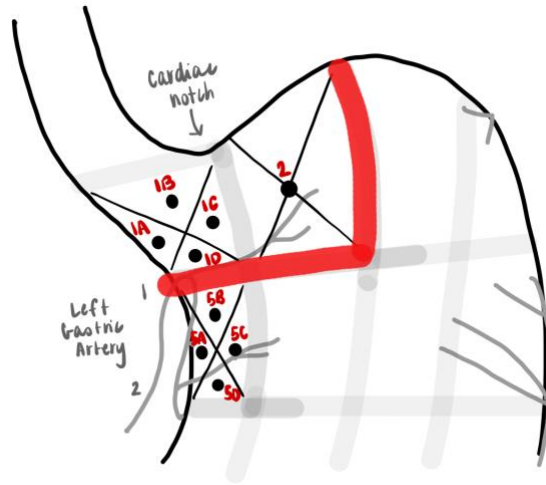


**Figure 11. Recommended gastric pouch location and dimensions. Gastric pouch should include segment 1 and 2. Recommendation for the horizontal grid line is the first branch of the left gastric artery, and the vertical grid line is 1/3 distance from the cardiac notch to greater curvature.**



**Figure 12. Recommended gastric pouch location and dimensions, illustrated on a cadaveric stomach. Recommendation for the horizontal grid line is the first branch of the left gastric artery, and the vertical grid line is 1/3 distance from the cardiac notch to greater curvature.**

While traditionally, surgeons opt to extend the gastric pouch vertically into the lesser curvature, it has become apparent based on this study, and previous work,<sup>7</sup> that the lesser curvature contains a high density of parietal cells. Limiting the amount to which the pouch extends into the lesser curvature would be beneficial for minimizing the number of parietal cells contained in the gastric pouch.

Segment 2, the proximal fundus, appears to contain a minimal number of parietal cells, and this region has a higher likelihood of containing SSNK epithelium compared to other stomach segments. Segment 2 could be included in the dimensions of the pouch. The fundus of the stomach by nature has elastic properties, which may be a source of concern for some surgeons who are worried about the gastric pouch dilating significantly over time. However, extending the horizontal pouch to only include section 2, which is 1/3 distance from the cardiac notch to the greater curvature (a few centimeters at most), would only be inclusive of the fundus region just adjacent to the GEJ, and would still be excluding the majority of the fundus, largely mitigating the ability of the pouch to stretch. Further experiments on the elastic nature of the proximal fundus would be beneficial in confirming the success of this surgical modification.

To conclude, our recommendation for the optimal size and location of the gastric pouch, according to standardized anatomical landmarks, is the *first branch of the left gastric artery* as the horizontal dimension, *1/3 distance from the cardiac notch to the greater curvature* as the vertical dimension, at most. This horizontal pouch based on the first branch of the left gastric artery will take advantage of two characteristics of segments 1 and 2; i) more likely to find SSNK epithelium (thus, no parietal cells), and ii) lower density of parietal cells, as compared to the distal lesser curvature, based on general trends in the data and visual analysis of histological images. We recommend excluding segment 5 from the pouch, avoiding extending the pouch vertically into the lesser curvature. This will minimize the number of parietal cells present in the gastric

pouch, thus limiting the ability of the pouch to produce acid, and reducing the incidence of marginal ulceration in patients undergoing gastric bypass surgery.

### **Future Directions**

This study utilized punch biopsies to obtain tissue from the stomach. In the future, an alternative approach would be to obtain larger biopsies, such as leaving the esophagus and proximal stomach intact, to look at the histology of the ‘transition zone’, similar to the study done by Stojisic et al.<sup>14</sup> We could then observe where the stratified squamous non-keratinizing epithelium of the esophagus stops, and there the oxyntic mucosa of the stomach begins. This transition zone could potentially allude to the inferior border of the gastric pouch.

Due to small sample size, and normalized parietal nuclei counts not being normally distributed, we were unable to run an ANOVA and post-hoc test, thus we are not able to determine which stomach segments in particular are significantly different than others. According to the Chi-Square Goodness of Fit test, stomach segments are significantly different from the expected value, being that all segments have the same normalized number of parietal nuclei. In the future, increasing the sample size would likely lead to more insightful findings on specifically which segments have fewer parietal nuclei than others. Although, increasing sample size would be difficult based on availability of cadaveric tissue; transitioning to animal models might be a solution to increase sample size for future experiments.

Initially, following the original schematic, we biopsied the entire stomach, taking 54 segments/cadaveric stomach. For the purposes of this study, we chose to only analyze

stomach segments in the region of interest for gastric bypass pouch (9 segments/stomach). We still do not know if parietal cell density is equal across the entire stomach, future studies could look to answer that question.

As mentioned previously, these findings of parietal cell density in various stomach segments were based on the assumption of normal stomach health in cadaveric subjects. Future experiments could explore parietal cell distribution based on disease state, such as GERD, ulcerative colitis or other inflammatory diseases.

### **Strengths and Weaknesses**

A strength of this study was the ability to use human tissue as opposed to animal models, in that the findings could be more generalizable. In the same vein, using human cadaveric tissue is a potential weakness of this study, in that the tissue is not in optimal condition for testing. Cadaveric tissue has been shown to be histologically reliable, in that tissue from embalmed cadavers are reported to be of good or satisfactory quality<sup>16</sup>. The type or quality of embalming, length of time the cadaver has been embalmed, and/or the organ from which the tissue is obtained are all factors that can impact the quality of the histological samples<sup>16</sup>. In the future, repeating this study with animal models or with unembalmed human tissue could offer a more complete picture.

## BIBLIOGRAPHY

- 1 Wolfe BM, Kvach E, Eckel RH. Treatment of Obesity: Weight Loss and Bariatric Surgery. *Circulation Research* 2016;**118**:1844–55.
- 2 Buchwald H, Avidor Y, Braunwald E, Jensen MD, Pories W, Fahrbach K, *et al.* Bariatric surgery: a systematic review and meta-analysis. *Journal of the American Medical Association* 2004;**292**:1724–37.
- 3 Seeras K, Acho RJ, Lopez PP. Roux-en-Y Gastric Bypass Chronic Complications. *StatPearls*. Treasure Island (FL): StatPearls Publishing; 2021.
- 4 Palermo M, Acquafresca PA, Rogula T, Duza GE, Serra E. Late surgical complications after gastric by-pass: a literature review. *Brazilian Archives of Digestive Surgery* 2015;**28**:139–43.
- 5 Allen A, Flemstrom G, Garner A, Kivilaakso E. Gastroduodenal mucosal protection. *Physiological Reviews* 1993:823–57.
- 6 Siilin H, Wanders A, Gustavsson S, Sundbom M. The proximal gastric pouch invariably contains acid-producing parietal cells in Roux-en-Y gastric bypass. *Obesity Surgery* 2005;**15**:771–7.
- 7 Sapala JA, Wood MH, Sapala MA, Schuhknecht MP, Flake TM Jr. The micropouch gastric bypass: technical considerations in primary and revisionary operations. *Obesity Surgery* 2001;**11**:3–17.
- 8 Roberts K, Duffy A, Kaufman J, Burrell M, Dziura J, Bell R. Size matters: gastric pouch size correlates with weight loss after laparoscopic Roux-en-Y gastric bypass. *Surgical Endoscopy* 2007;**21**:1397–402.
- 9 Clapp B. Anatomic landmarks in the sleeve gastrectomy. *Journal of the Society of Laparoendoscopic Surgeons* 2013;**17**:388–9.
- 10 Otsu N. A Threshold Selection Method from Gray-Level Histograms. *IEEE Transactions on Systems, Man, and Cybernetics* 1979:62–6.  
<https://doi.org/10.1109/tsmc.1979.4310076>.
- 11 van der Walt S, Schönberger JL, Nunez-Iglesias J, Boulogne F, Warner JD, Yager N, *et al.* scikit-image: image processing in Python. *PeerJ* 2014;**2**:e453.
- 12 Li CH, Tam PKS. An iterative algorithm for minimum cross entropy thresholding. *Pattern Recognition Letters* 1998;**19**:771–6.

- 13 Zhang N, Maffei A, Cerabona T, Pahuja A, Omana J, Kaul A. Reduction in obesity-related comorbidities: is gastric bypass better than sleeve gastrectomy? *Surgical Endoscopy* 2013;**27**:1273–80.
- 14 Stojic ZM, Stevanovic RM, Stojanovic MM, Stanojevic AD, Bacetic DT. Histological features of gastric cardia in adults: an autopsy study. *Journal of Gastrointestinal and Liver Diseases* 2011;**20**:13–8.
- 15 Lowe D, Kudaravalli P, Hsu R. Barrett Metaplasia. *StatPearls*. Treasure Island (FL): StatPearls Publishing; 2022.
- 16 Abuhaimed AK, Almulhim AM, Alarfaj FA, Almustafa SS, Alkhater KM, Al Yousef MJ, *et al*. Histologic Reliability of Tissues from Embalmed Cadavers: Can They be Useful in Medical Education? *Saudi Journal of Medicine & Medical Sciences* 2020;**8**:208–12.

**CURRICULUM VITAE**

